JOURNAL OF VIROLOGY, Jan. 2005, p. 1262–1270 Vol. 79, No. 2
0022-538X/05/$08.00+0 doi:10.1128/JVI.79.2.1262–1270.2005

Influenza A Viruses with Mutations in the M1 Helix Six Domain Display a Wide Variety of Morphological Phenotypes

Laura M. Burleigh,[1,2] Lesley J. Calder,[2] John J. Skehel,[2] and David A. Steinhauer[1,2]*

Department of Microbiology and Immunology, Emory University School of Medicine, Atlanta, Georgia,[1] and Division of Virology, National Institute for Medical Research, London, United Kingdom[2]

Received 29 June 2004/Accepted 16 August 2004

Several functions required for the replication of influenza A viruses have been attributed to the viral matrix protein (M1), and a number of studies have focused on a region of the M1 protein designated "helix six." This region contains an exposed positively charged stretch of amino acids, including the motif 101-RKLKR-105, which has been identified as a nuclear localization signal, but several studies suggest that this domain is also involved in functions such as binding to the ribonucleoprotein genome segments (RNPs), membrane association, interaction with the viral nuclear export protein, and virus assembly. In order to define M1 functions in more detail, a series of mutants containing alanine substitutions in the helix six region were generated in A/WSN/33 virus. These were analyzed for RNP-binding function, their capacity to incorporate into infectious viruses by using reverse genetics, the replication properties of rescued viruses, and the morphological phenotypes of the mutant virus particles. The most notable effect that was identified concerned single amino acid substitution mutants that caused significant alterations to the morphology of budded viruses. Whereas A/WSN/33 virus generally forms particles that are predominantly spherical, observations made by negative stain electron microscopy showed that several of the mutant virions, such as K95A, K98A, R101A, and K102A, display a wide range of shapes and sizes that varied in a temperature-dependent manner. The K102A mutant is particularly interesting in that it can form extended filamentous particles. These results support the proposition that the helix six domain is involved in the process of virus assembly.

The influenza A virus M1 protein is the most abundant structural component of the virion, and electron microscopy studies of influenza virus A particles show that M1 forms a shell at the internal surface of the viral membrane (6, 39, 47). The functions of M1 have been studied extensively, and it has been implicated in a variety of roles in the virus life cycle that include RNA and RNP binding (4, 5, 14, 41, 43, 51, 52, 55, 57), transcription inhibition (5, 14, 52, 58, 62), and control of RNP nuclear import and export (8, 21, 34, 35, 53, 54). In addition, cell fractionation experiments with expressed M1 protein or virus-infected cells show it to exist in both soluble and membrane-bound forms. There are examples in which coexpression of the viral glycoproteins was found to stimulate membrane association overall (15), but this was not noted in other reports (30, 59). It is also thought that M1 recruitment to lipid raft microdomains on the apical surface of polarized epithelial cells, the site of influenza virus budding, is stimulated by the presence of the intact glycoproteins (1, 3, 61). Taken together, most of the results support the long held hypothesis that M1 can associate with RNPs on one hand and viral glycoproteins on the other and plays a prominent role in virus assembly.

Analogous matrix proteins are considered important for the process of assembly and budding for a variety of unrelated viruses. With many of these, studies on the formation of virus-like particles (VLPs) indicate that two or more viral proteins appear to be required for efficient budding and particle formation (46). With others, such as vesicular stomatitis virus, Ebola virus, and retroviruses, expression of the matrix protein alone (Gag in the case of retroviruses) can lead to the formation of VLPs (12, 17, 24, 26, 27, 50). VLP studies with influenza virus also identify the M1 protein as a vital component for efficient virus assembly. In studies with baculovirus or vaccinia-T7 expressed influenza virus proteins, VLPs have been detected only when the combination of proteins analyzed included M1 (18, 31), and in some cases such particles were observed after the expression of M1 alone (18), supporting the concept that M1 is essential for the process of assembly and budding.

The M1 protein is encoded by genome segment 7, which also encodes the M2 protein by using a spliced mRNA. M1 contains 252 amino acids, but high-resolution structural information is currently restricted to the N-terminal two-thirds of the protein (residues 1 to 164). X-ray crystal structures of this portion of M1 have been solved at both pH 4.0 and pH 7.0 (2, 20, 48), and each shows the M1 monomer to be composed of two four-helix bundles as depicted in Fig. 1. To date, information on the atomic structure of the M1 C-terminal domain (residues 165 to 252) is not available since this region is quite susceptible to degradation by endogenous proteases encountered during protein preparation (2). Two models for the oligomeric structure of M1 have been proposed. In one, based partly on crystals produced at pH 4.0 (48), it is suggested that dimeric interactions may be the basis for oligomerization of M1 to form a shell (20). Alternatively, a model has been proposed in which M1 assembles through the interaction of positive charges on one face of a monomer with negative charges on the opposite face of an adjacent M1 monomer (2).

Influenza A virions can exhibit a remarkable degree of struc-

* Corresponding author. Present address: Department of Microbiology and Immunology, Emory University School of Medicine, Rollins Research Center, 1510 Clifton Rd., Atlanta, GA 30322. Phone: (404) 712-8542. Fax: (404) 727-3659. E-mail: steinhauer@microbio.emory.edu.

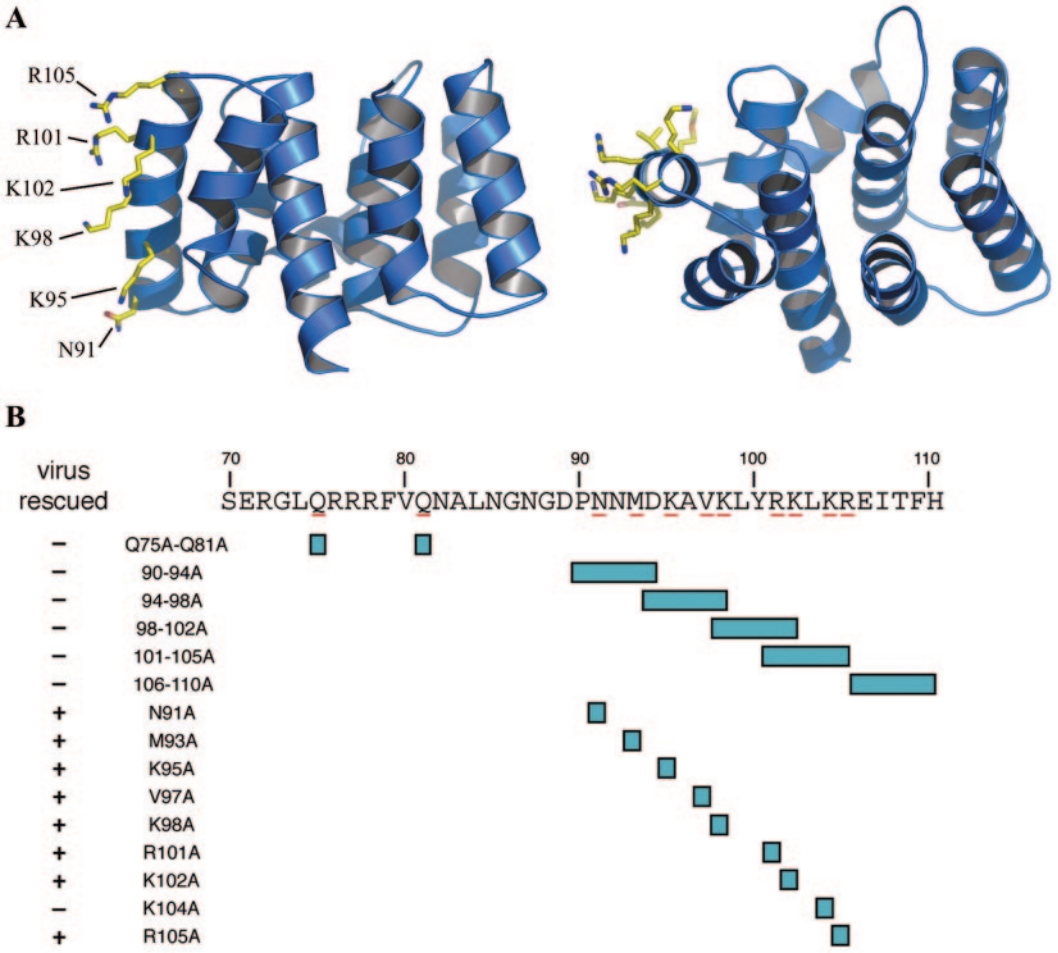

FIG. 1. (A) Ribbon diagram of the M1 protein structure. The right panel is rotated by 90° relative to the left panel, such that the top of helix six in the left panel orients toward the reader in the right panel. The residues indicated in yellow are (bottom to top, left panel; back to front, right panel) N91, K95, K98, R101, K102, and R105. (B) Schematic diagram of mutations introduced into amino acids 75 to 110 of the M1 gene and results of virus rescue. Blue boxes indicate residues mutated to alanine.

tural variation. Whereas most laboratory strains such as A/WSN/33 (WSN) display spherical or kidney-shaped morphologies with diameters of approximately 80 to 120 nm, freshly derived clinical isolates are notable for their propensity to form filamentous particles (9–11, 37). Laboratory passage of filamentous viruses often leads to progressive morphological changes to spherical forms (9, 28); however, there are examples of well-established laboratory strains such as A/Udorn/72 (Udorn) that maintain a predominantly filamentous phenotype (22, 44).

Several studies have documented a direct linkage between viral genotype and morphological phenotype. Genetic studies on the cytoplasmic tail domains of the hemagglutinin (HA) and neuraminidase (NA) glycoproteins show that truncation of either of these can lead to a change in morphology (25, 36). A mutant containing truncations in both the HA and NA cytoplasmic tail domains was shown to display a particularly exaggerated phenotype, containing large bulbous domains linked by long, narrow stretches (25). There are also several examples in which the M1 protein has been demonstrated as a determinant of virion morphology (7, 13, 22, 29, 44, 49). Studies on the Udorn strain showed that mutants selected to replicate in the presence of a monoclonal antibody directed against the extracellular region of the M2 protein can contain changes not only in the M2 protein but also in M1, and the M1 mutation correlates with morphology (44). Bourmakina and Garcia-Sastre used reverse genetics to make viruses with combinations of Udorn and WSN M1 and M2 genes on a WSN background and determined that residues in each domain of M1 can individually be involved in morphology changes (7). A similar reverse genetics approach has been used to verify that the M1 gene, and in particular the specific combination of amino acids at positions 41, 95, and 218 controls morphology in the genetic background of the filamentous virus A/Victoria/3/75 (13). In addition, it has recently been reported that for influenza virus C, residue 24 of M1 can influence virion morphology (38). Another study of several mutants in the helix six domain of WSN M1 generated by reverse genetics indicated that changes at position 101 can affect virus morphology (23). That study also provided evidence that the 100-YRKL-103 motif in helix six may function as a late domain (23) and, as such, may be involved in interactions with cellular proteins required for the

processes of viral budding and release (for a review, see reference 42).

The present study focuses on mutants derived by reverse genetics to define in more detail the role of the helix six domain in the virus replication cycle and, in particular, virus assembly. They provide a more detailed structural examination of the virus morphology of M1 mutants than previously reported and reveal that a wide variety of morphological phenotypes can result from single residue substitutions in this region, reinforcing the concept that M1 has a prominent role in the assembly of influenza A viruses.

MATERIALS AND METHODS

Cells and viruses. Madin-Darby canine kidney (MDCK) and 293T human embryonic kidney cells were maintained in Dulbecco modified Eagle medium (DMEM; Gibco) supplemented with 5% fetal calf serum (PAA Laboratories) and 100 U of penicillin and streptomycin (Gibco)/ml. Influenza A/WSN/33 virus was propagated in MDCK cells at a multiplicity of infection of ≤0.01.

Generation of infectious influenza viruses by reverse genetics. Mutant viruses (A/WSN/33 strain) were generated by using the reverse genetics system described by Neumann et al. (40), and plasmids were kindly provided by Y. Kawaoka. M1 gene mutations were introduced into the pPolI-WSN-M RNA expression vector by using a QuikChange kit (Stratagene). Sequence analysis confirmed that only the specifically introduced mutations were present in the plasmids. 293T cells at approximately 70% confluence in 60-mm dishes were transfected with eight RNA expression plasmids, corresponding to the eight viral segments, and protein expression plasmids for all viral proteins with the exception of NS1. DNA (2 μg of each plasmid except for pcDNA 787 PA, pCAGGS WSN-M1, pCA NS2, and pEP24C M2 for which 0.2, 4, 0.6, and 0.06 μg, respectively, were used) was diluted in 150 μl of Optimem (Gibco), mixed with 60 μl of Superfect (Qiagen), and incubated for 15 min before it was added to 293T cells maintained in DMEM. Medium was replaced 3 h later, and cells were incubated at 33°C. At 2 to 3 days posttransfection cell supernatants were treated with 2.5 μg of trypsin/ml and either titrated directly by plaque assay or amplified on MDCK cells.

Plaque assay. Confluent MDCK cells in 35-mm dishes were washed with serum-free DMEM, and serial dilutions of virus were adsorbed onto cells for 30 min at room temperature. Unadsorbed viruses were removed by washing with serum-free DMEM, and cells were overlaid with 2 ml of overlay medium (2× DMEM supplemented with 160 μg of DEAE-dextran/ml, 20 mM glutamine, 2.5 μg of trypsin/ml, and 1% noble agar). After 3 days of incubation at 33, 37, or 38.5°C cells were fixed with 0.25% glutaraldehyde for 30 min at room temperature. The overlay was removed, and cells were blocked with 3% bovine serum albumin (BSA) in phosphate-buffered saline (PBS), incubated with anti-WSN polyclonal antibody (1:500 in 3% BSA-PBS) for 1 h, washed, and incubated with 1 ml of protein A-horseradish peroxidase (Bio-Rad) diluted 1:1,000 in 3% BSA-PBS for an hour. Plaques were visualized after the addition of 1 ml of a hydrogen peroxide–4-chloro-1-naphthol solution.

RNP purification and binding to M1. RNPs were purified as described previously (45). Egg-grown NWS virus (1 mg/ml in PBS) was disrupted by incubation at pH 4.8, followed by the addition of 0.5% lubrol for 1 h at 25°C. RNPs were pelleted at 150,000 × *g* for 15 min, resuspended in PBS (pH 4.8), and sedimented through a 10 to 40% sucrose gradient containing 0.5% *n*-octyl-β-D-glucopyranoside for 3 h at 75,000 × *g* and 4°C. The RNP pellet was resuspended in 10 mM Tris (pH 7.4). Sodium dodecyl sulfate-polyacrylamide gel electrophoresis (SDS-PAGE) and Coomassie blue staining showed that residual M1 was undetectable (Fig. 2B). Mutant M1 proteins labeled with ^{35}S were generated by using the TNT T7 Quick Transcription and Translation System (Promega). SDS-PAGE analysis showed that the proteins were expressed and that their migration patterns indicated the appropriate molecular weights in each case. The labeled M1 was washed with 10 mM Tris to remove excess ^{35}S. A total of 100,000 cpm of each M1 protein was incubated with 10 μg of RNP in 100 μl of binding buffer (10 mM Tris [pH 6.8], 150 mM NaCl, and 1% NP-40) at room temperature for 1 h. RNPs and any associated M1 were pelleted through 150 μl of 20% glycerol in binding buffer at 14,000 × *g* for 15 min, and the M1 content of the pellet was analyzed by scintillation counting.

Polypeptide composition analysis. Supernatants of WSN-infected MDCK cells were clarified by centrifugation at 3,000 × *g* for 10 min. Viruses were harvested by centrifugation at 85,000 × *g* for 90 min and further purified on a 30 to 60% sucrose gradient. Virus-containing fractions were concentrated ~10-fold by using a 10-kDa cutoff Vivaspin concentrator (Vivascience) and then analyzed by 12% PAGE. Coomassie blue-stained gels were scanned by using a GelDoc system (Bio-Rad), and the band density was determined by using Quantity One software (Bio-Rad).

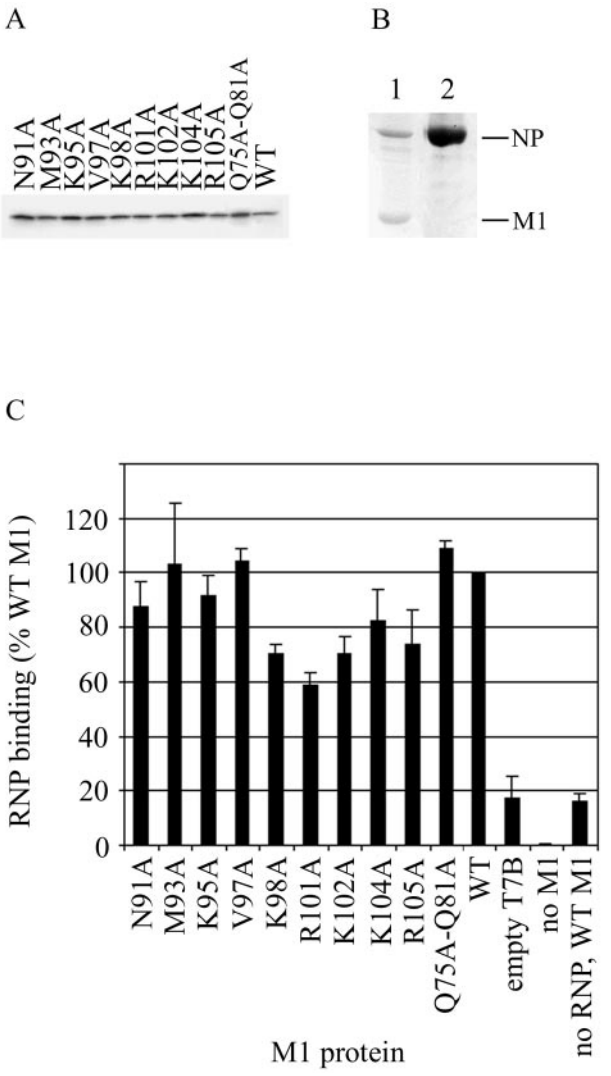

FIG. 2. (A) Autoradiograph of in vitro-transcribed and translated M1 proteins. (B) SDS-PAGE analysis and Coomassie blue staining of RNP purification. Lane 1, untreated virus; lane 2, RNP purified by low-pH and detergent treatment. (C) Binding of mutant and wild-type ^{35}S-labeled M1 to RNP. A total of 100,000 cpm of M1 was incubated with 10 μg of RNP. RNPs were pelleted through 20% glycerol, and the M1 associated with RNP was quantitated. Experiments were carried out three times.

Electron microscopy. Mutant and wild-type viruses grown in MDCK cells at both 33 and 37°C were harvested from the supernatants by centrifugation at 85,000 × *g* for 90 min and washed three times in PBS. Viruses were stained with 1% sodium silicotungstate and examined under low-dose, high-resolution conditions.

RESULTS AND DISCUSSION

RNP binding. To explore the role of the helix six domain for virus replication in more detail, we generated and analyzed a series of mutants in this region (illustrated in Fig. 1A). The mutations that were made include several single site substitu-

TABLE 1. Titer of rescued viruses in 293T cell supernatants[a]

M1 protein	Virus titer (PFU/ml)
N91A	1.00×10^4
M93A	2.00×10^5
K95A	1.50×10^5
V97A	3.00×10^2
K98A	4.50×10^3
R101A	2.50×10^5
K102A	3.50×10^5
R105A	2.65×10^4
Wild type	7.50×10^7

[a] Plaque assays were carried out at 33°C. Titers are the average of three experiments.

TABLE 2. Titers of wild-type and mutant viruses at various temperatures[a]

M1 protein	Virus titer (PFU/ml) at:		
	33.0°C	37.0°C	38.5°C
N91A	2.20×10^5	2.10×10^5	1.20×10^5
M93A	8.17×10^4	1.21×10^5	2.23×10^4
K95A	8.25×10^5	6.15×10^5	5.54×10^4
V97A	2.68×10^4	1.57×10^4	3.00×10^3
K98A	5.01×10^5	1.67×10^5	1.85×10^5
R101A	3.34×10^4	2.18×10^4	5.00×10^1
K102A	1.28×10^4	1.53×10^4	2.00×10^3
R105A	2.80×10^5	7.00×10^4	1.02×10^5
Wild type	2.75×10^6	2.50×10^6	8.40×10^6

[a] Titers are the average of three experiments.

tions to alanine, a double residue substitution corresponding to residues suggested to be involved in dimer interactions in the pH 4.0 crystal structure (48), and mutants in which five contiguous residues were mutated to alanine (Fig. 1B). The residues 101-RKLKR-105 in this exposed helix constitute a putative nuclear localization signal (56), and mutagenesis studies have suggested that these and surrounding residues may be important for RNA and RNP binding (5, 14, 57). However, other studies with *Escherichia coli*-expressed M1 proteins indicate that the C-terminal portion of the protein that is not represented in the crystal structure is responsible for RNP binding (5). We expressed the M1 single substitution mutants outlined in Fig. 1B by using a mammalian cell expression system and analyzed them for their capacity to bind to low-pH detergent-extracted viral RNPs. Using this system the migration patterns of expressed proteins indicated the appropriate molecular weights in each case (Fig. 2A). RNPs were purified from egg-grown virus by using low pH and detergent (45), and residual M1 was undetectable (Fig. 2B). RNP binding analysis with equal quantities of each radiolabeled single substitution mutant showed that binding of the mutants with changes at positions 91, 93, 95, and 97 was similar to the binding of the wild type, as was binding of the Q75A-Q81A double mutant. The RNP binding of the alanine substitution mutants at positions 98, 101, 102, 104, and 105 were slightly reduced, ranging from 60% for R101K to 82% for the K104A mutant (Fig. 2C). Overall, although our results do not rule out a possible role for helix six residues in RNP binding, either directly or indirectly, they fail to provide compelling evidence that any of the particular amino acids that were mutated are critical for RNP binding.

Generation of infectious influenza viruses by reverse genetics. In order to analyze the M1 mutants in the context of the virus life cycle, we attempted to incorporate the mutations detailed in Fig. 1B into infectious viruses by using the plasmid-based system described previously by Neumann et al. (40). Plasmids encoding genomic RNAs and the structural proteins of the virus were transfected into 293T cells. Wild-type virus titers on the order of 10^7 PFU/ml were routinely obtained from transfected 293T cells, whereas the rescue of mutant viruses was significantly less efficient. None of the viruses containing multiple alanine substitutions was rescued, nor was the K104A virus (Fig. 1B). Among the viruses that were generated, initial titers of the M1 mutants from 293T supernatants were reduced by 2 to 5 orders of magnitude relative to the wild type (Table 1). We also observed that it was difficult to plaque the M1 mutant viruses from the 293T cell supernatants at 37°C, so the titers shown in Table 1 were initially obtained at 33°C. Viruses containing the K104A mutation and the multiple substitution mutations were not recovered after repeated rescue attempts at both 33 and 37°C (Fig. 1B). In general, our results are consistent with recent reports regarding the rescue of viruses containing mutations in helix six (23, 32), although in several examples the positions and individual substitutions chosen for examination differed. In those studies and in the present study, no viruses with changes at position 104 were rescued; however, we were able to rescue the K105A mutant, which proved to be problematic in previous studies, demonstrating that a positively charged residue at position 105 is not an absolute requirement for virus infectivity.

Our observation that it was initially difficult to obtain plaques at 37°C with M1 mutants suggested that they might have temperature-sensitive phenotypes. To assess this, the viruses were analyzed for replication properties at 33, 37, and 38.5°C (Table 2). In each case, little difference in replication efficiency was observed between 33 and 37°C. Several of the mutants displayed a slight decrease in titer ($\leq$1 log) when titers were determined at 38.5°C, but only the R101A mutant, which exhibited a decrease in titer by approximately 3 logs, could reasonably be considered temperature sensitive under the conditions tested. The K102A mutant displayed a reduced plaque size at all temperatures, but the plaque morphology of all other mutant viruses was comparable to that of the wild type and did not vary with increased temperature (Fig. 3).

The genetic stability of the M1 mutations was examined by multiple passage of the viruses on MDCK cells at both 33°C and 38.5°C. After eight passages at each temperature, sequence analysis of the M1 coding region showed that all of the introduced mutations remained present. The only other mutation detected was from the K98A mutant passaged at 38.5°C, which contained an additional change from isoleucine to methionine at residue 131. We conclude that although none of the viruses replicate as well as the wild type at any temperature, in general, the mutants are not temperature sensitive as defined in the classical sense (33), nor does plaque size serve as a useful indicator of replication efficiency.

Morphology of rescued viruses. Influenza virus assembly remains a process that is not well understood, but much of what is known derives from studies on virus morphology. We

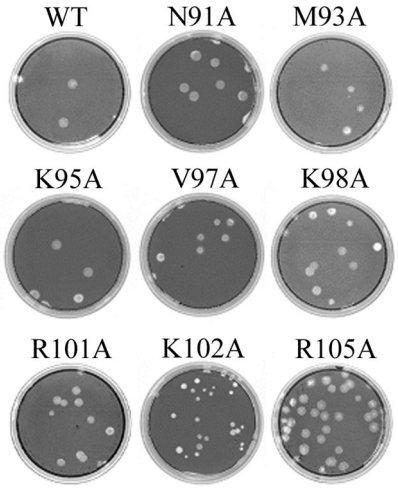

FIG. 3. Plaque morphology of mutant and wild-type viruses. MDCK cells were infected at equal multiplicities of infection. After incubation for 3 days at 37°C, the cells were stained with crystal violet. No difference in plaque size was observed when cells were incubated at 33 and 38.5°C.

analyzed the morphology of our viruses by negative stain electron microscopy of passage 2 stocks grown at either 33 or 37°C. We found that in broad terms, we could classify the mutants into two groups. The N91A, M93A, V97A, and R105A mutants resemble wild-type virus in size and appearance both at 33 and at 37°C (Fig. 4); however, as shown in Fig. 5, the K95A, K98A, R101A, and K102A mutants have altered sizes and shapes relative to typical influenza WSN virions (Udorn virus is also shown as an example of a well-characterized filamentous virus). It should be pointed out that even within the populations of viruses with altered morphology, a proportion of spherical virions can often be observed (Fig. 5). This is not unusual and has been observed, for example, in preparations of Udorn virus (44) and mutant viruses containing glycoprotein deletions in their cytoplasmic tail domains (60). The mutants that resemble wild type are relatively spherical, with well ordered HA spikes on the surface. However, for the viruses with altered morphology, differences in appearance were observed to be dependent on temperature in some cases (Fig. 5). At 33°C, K95A virions are enlarged and are either spherical or amorphous. At 37°C

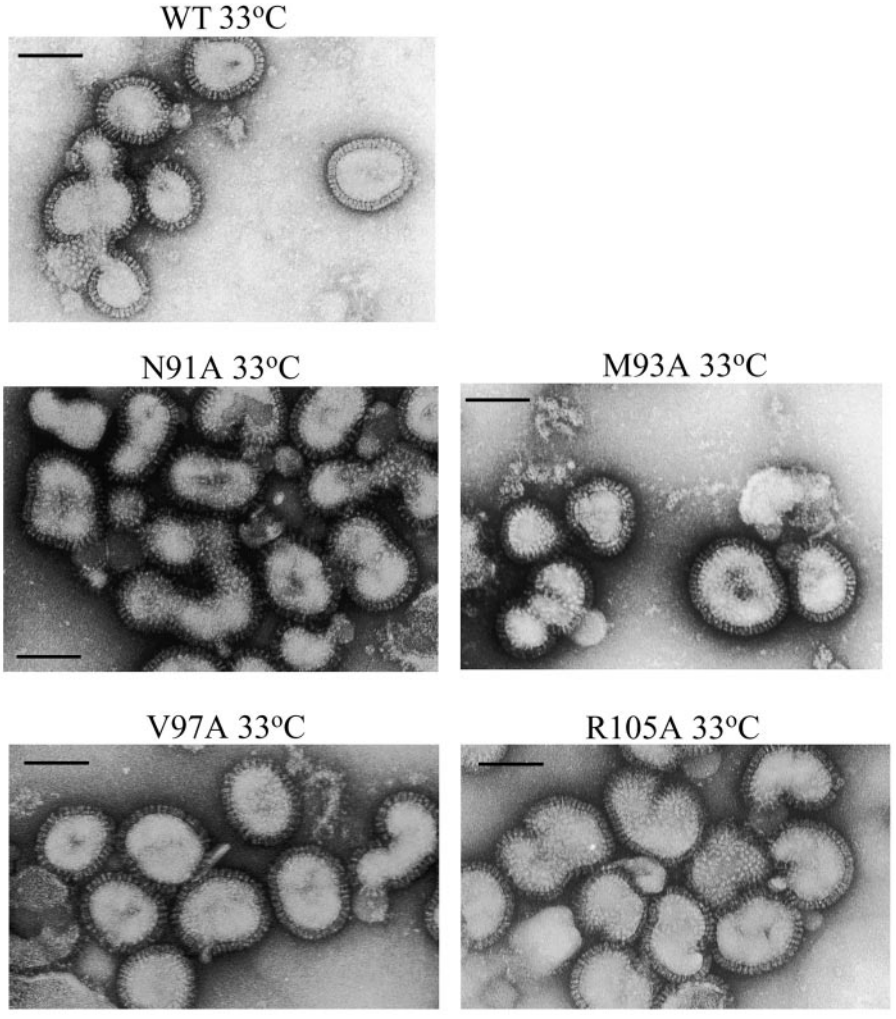

FIG. 4. Negative stain electron microscopy of wild-type viruses and mutant viruses with wild type-like morphology at 33°C. Morphology did not vary at 37°C (data not shown). The scale bars represent 100 nm. Viruses were stained with 1% sodium silicotungstate and examined under low-dose, high-resolution conditions.

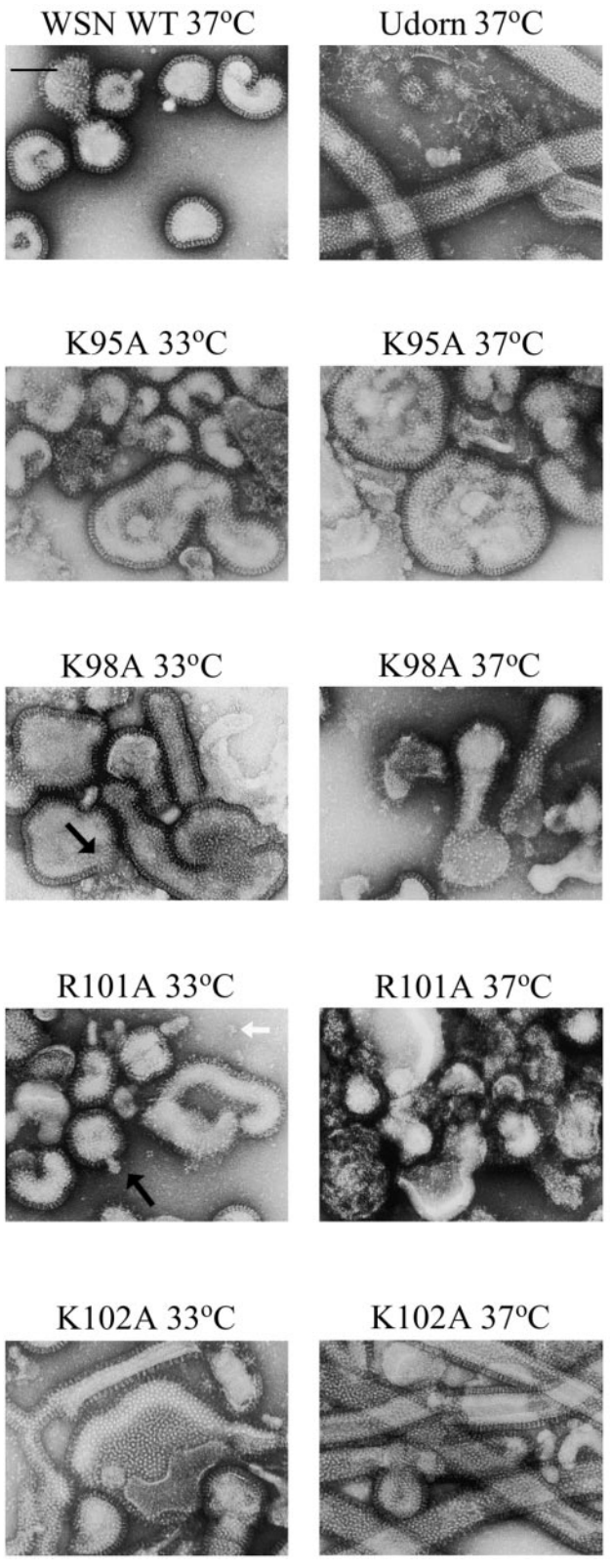

FIG. 5. Negative stain electron microscopy of mutant viruses with an altered morphology at 33 and 37°C. A/Udorn/72 virus is shown as an example of filamentous morphology. Black arrows indicate areas of membrane disruption; white arrows indicate shed HA. The scale bars represent 100 nm. Viruses were stained with 1% sodium silicotungstate and examined under low-dose, high-resolution conditions.

the virions are generally spherical but are greatly enlarged, with a diameter approximately three times that of wild type. K98A forms enlarged and irregularly shaped virions at 33°C, with some disruption of membranes. When grown at 37°C K98A has a diameter similar to wild-type virus but the virions are often extended and terminate in bulbous regions. The R101A mutants at 33°C are similar in size to the wild-type virus but display a greater proportion of pleiomorphic virions, as well as disruptions in the membrane and some HA shedding from the surface. The phenotype at 37°C shows a greater extent of particle disruption and altered HA. The K102A grown at 33°C produces a mixture of virion morphologies. Some particles are small and roughly spherical, but many are enlarged or elongated with occasional branching, and a few virions form regular filaments. At 37°C the K102A mutant forms highly filamentous particles that are much more regular in appearance than the extended structures seen at 33°C or with other mutants. The filaments have a constant diameter and intact HA, indicating that they are not formed from fusion of several spherical virions, and when M1 is visible it is arranged in a regular and undisrupted "fingerprint" pattern, typical of filamentous virus strains (Fig. 6A). This is in contrast to the appearance of M1 in spherical virions, where the fingerprint pattern is often discontinuous (45). Furthermore, lower magnification shows that the filaments often extend more than 1 μm in length (Fig. 6B). These factors provide evidence that K102A filaments are distinct from the elongated virions observed for other mutants and more closely resemble filamentous strains of influenza virus such as Udorn.

Interestingly, the mutants displaying an altered morphology do not replicate at levels significantly different than those with a wild-type-like appearance at either temperature (Tables 1 and 2). This is interesting since some studies have found that Udorn variants with spherical morphology can replicate to higher levels than those which retain the filamentous phenotype (44). The protein composition of purified wild-type and K102A virions was examined by PAGE and Coomassie blue staining (Fig. 7), and little difference was observed. In some instances filamentous virions have higher M1/NP ratios than their counterpart spherical particles, but these values have been shown to vary depending on the mutant analyzed (44). Ratios of the viral proteins in lysates of cells infected with wild type and the filamentous mutant K102A were also similar, although the overall levels of viral proteins were reduced by ca. 50% for the mutant (data not shown). This and the filamentous nature of the mutant viruses may explain, in part, the reduced titers observed relative to the wild type.

The altered morphologies of several of the helix six mutants suggest that this region of M1 may be involved in the process of virion assembly. Although virus morphology can be linked to genetic changes in several viral components (25, 36, 44), the M1 gene appears to be the most prominent for controlling morphology. Bourmakina and Garcia-Sastre (7) generated viruses based on the Udorn M1 with a WSN background to show that the M1 gene confers the morphological phenotype. Residues 95 and 204 were found to be particularly critical for the formation of filamentous virus particles, since Udorn-to-WSN M1 substitutions at these positions individually conferred a reduction in filamentous phenotype. Residue 95 is in the same region as the mutants analyzed in our study and was one of the

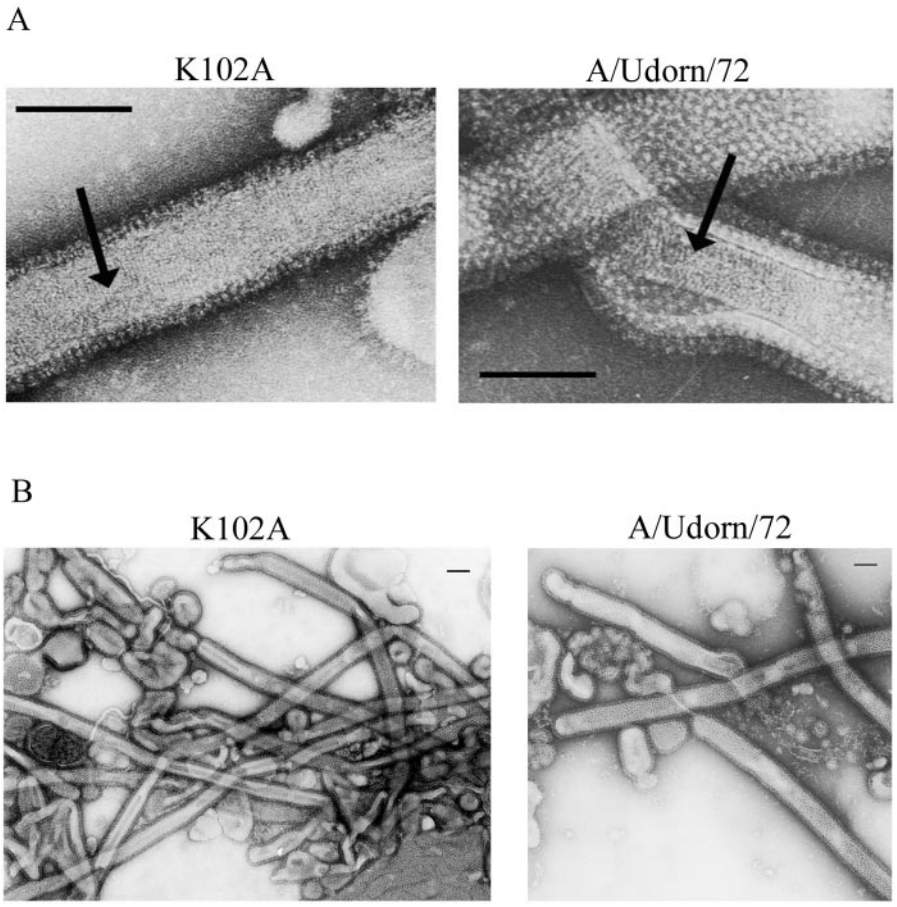

FIG. 6. (A) M1 arrangement in filamentous K102A mutants and in A/Udorn/72 virions. Arrows indicate areas where the M1 arrangement is visible. (B) Reduced magnification of K102A mutant and Udorn, showing filaments >1 μm in length. Scale bars, 100 nm. Viruses were stained with 1% sodium silicotungstate and examined under low-dose, high-resolution conditions.

residues that we found to affect morphology. Residue 204 is in the C-terminal domain for which we have little structural information. The study by Roberts et al. described above demonstrated that the amino acid at position 41 can also be a determinant of filamentous morphology (44). Nayak and coworkers (23) made mutant viruses at several positions of the M1 helix six domain and analyzed a few by thin-section transmission electron microscopy. The most striking morphological phenotype that they showed involved the R101A virus, for which they observed several elongated particles and, consistent with our 37°C results with the same mutant, noted a number of disrupted empty particles. Overall, the data suggest that mutations in several regions of M1 have the potential to relate to changes in morphological phenotype. Our results are consistent with the studies cited above, but the relative increase in resolution of the electron micrographs presented here clearly shows the varied array of morphological phenotypes that can result from changes in the M1 helix six domain.

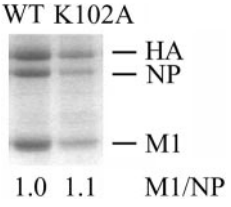

FIG. 7. Protein composition of wild-type and K102A virions. Virions were analyzed on a 12% polyacrylamide gel. The band density was determined by using Quantity One (Bio-Rad) software.

In addition, it has recently been proposed that residues 101-YRKL-103 in helix six of M1 may constitute a late domain (23). Late domains are motifs identified in the Gag proteins of various retroviruses and in the matrix proteins of rhabdoviruses and filoviruses that interact with the cellular proteins required for viral budding and release (for reviews, see references 16 and 42). Viruses with mutations in this domain frequently display a reduction in virion production, and thin-section electron micrographs of human immunodeficiency virus type 1 late domain mutants reveal virus particles that are not released in the normal fashion but are attached to the cell surface by a stalk-like structure (19). The unusual morphology of several of our mutants, in particular the appearance of the K98A mutant at 37°C, could be consistent with a defect in particle release; however, further studies are required to fully characterize the interactions occurring between viral and cellular components during budding.

Overall, our results support and extend many of the conclusions from previous studies on helix six mutations and on the relationship between M1 and virus morphology. The most notable finding of the present study is that at several positions along the helix six region of M1, the residue present can have significant effects on virus morphology, suggesting that this region plays an important role in the assembly process. The observation that filamentous viruses predominate in fresh clinical isolates suggests that in the host virus morphology may possibly be a determinant of infectivity and/or pathogenicity, and understanding the genetic basis of virus morphology may be important from a medical standpoint.

ACKNOWLEDGMENTS

We thank Rupert Russell for generating Fig. 1A and lab members and Dick Compans for critical comments on the manuscript.

This study was supported by the Medical Research Council (United Kingdom) and Public Health Service grants AI66870 and AI/EB53359 from the National Institutes of Health.

REFERENCES

1. **Ali, A., R. T. Avalos, E. Ponimaskin, and D. P. Nayak.** 2000. Influenza virus assembly: effect of influenza virus glycoproteins on the membrane association of M1 protein. J. Virol. **74:**8709–8719.
2. **Arzt, S., F. Baudin, A. Barge, P. Timmins, W. P. Burmeister, and R. W. Ruigrok.** 2001. Combined results from solution studies on intact influenza virus M1 protein and from a new crystal form of its N-terminal domain show that M1 is an elongated monomer. Virology **279:**439–446.
3. **Barman, S., A. Ali, E. K. Hui, L. Adhikary, and D. P. Nayak.** 2001. Transport of viral proteins to the apical membranes and interaction of matrix protein with glycoproteins in the assembly of influenza viruses. Virus Res. **77:**61–69.
4. **Baudin, F., C. Bach, S. Cusack, and R. W. Ruigrok.** 1994. Structure of influenza virus RNP. I. Influenza virus nucleoprotein melts secondary structure in panhandle RNA and exposes the bases to the solvent. EMBO J. **13:**3158–3165.
5. **Baudin, F., I. Petit, W. Weissenhorn, and R. W. Ruigrok.** 2001. In vitro dissection of the membrane and RNP binding activities of influenza virus M1 protein. Virology **281:**102–108.
6. **Booy, F. P., R. W. Ruigrok, and E. F. van Bruggen.** 1985. Electron microscopy of influenza virus. A comparison of negatively stained and ice-embedded particles. J. Mol. Biol. **184:**667–676.
7. **Bourmakina, S. V., and A. Garcia-Sastre.** 2003. Reverse genetics studies on the filamentous morphology of influenza A virus. J. Gen. Virol. **84:**517–527.
8. **Bui, M., G. Whittaker, and A. Helenius.** 1996. Effect of M1 protein and low pH on nuclear transport of influenza virus ribonucleoproteins. J. Virol. **70:**8391–8401.
9. **Choppin, P. W., J. S. Murphy, and I. Tamm.** 1960. Studies of two kinds of virus particles which comprise influenza A virus strains. III. Morphological and functional traits. J. Exp. Med. **112:**945–952.
10. **Chu, C. M., I. M. Dawson, and W. J. Elford.** 1949. Filamentous forms associated with newly isolated influenza virus. Lancet **i:**602–603.
11. **Cox, J. C., A. W. Hampson, and R. C. Hamilton.** 1980. An immunofluorescence study of influenza virus filament formation. Arch. Virol. **63:**275–284.
12. **Delchambre, M., D. Gheysen, D. Thines, C. Thiriart, E. Jacobs, E. Verdin, M. Horth, A. Burny, and F. Bex.** 1989. The GAG precursor of simian immunodeficiency virus assembles into virus-like particles. EMBO J. **8:**2653–2660.
13. **Elleman, C. J., and W. S. Barclay.** 2004. The M1 matrix protein controls the filamentous phenotype of influenza A virus. Virology **321:**144–153.
14. **Elster, C., K. Larsen, J. Gagnon, R. W. Ruigrok, and F. Baudin.** 1997. Influenza virus M1 protein binds to RNA through its nuclear localization signal. J. Gen. Virol. **78:**1589–1596.
15. **Enami, M., and K. Enami.** 1996. Influenza virus hemagglutinin and neuraminidase glycoproteins stimulate the membrane association of the matrix protein. J. Virol. **70:**6653–6657.
16. **Freed, E. O.** 2002. Viral late domains. J. Virol. **76:**4679–4687.
17. **Gheysen, D., E. Jacobs, F. de Foresta, C. Thiriart, M. Francotte, D. Thines, and M. De Wilde.** 1989. Assembly and release of HIV-1 precursor Pr55gag virus-like particles from recombinant baculovirus-infected insect cells. Cell **59:**103–112.
18. **Gomez-Puertas, P., C. Albo, E. Perez-Pastrana, A. Vivo, and A. Portela.** 2000. Influenza virus matrix protein is the major driving force in virus budding. J. Virol. **74:**11538–11547.
19. **Gottlinger, H. G., T. Dorfman, J. G. Sodroski, and W. A. Haseltine.** 1991. Effect of mutations affecting the p6 gag protein on human immunodeficiency virus particle release. Proc. Natl. Acad. Sci. USA **88:**3195–3199.
20. **Harris, A., F. Forouhar, S. Qiu, B. Sha, and M. Luo.** 2001. The crystal structure of the influenza matrix protein M1 at neutral pH: M1–M1 protein interfaces can rotate in the oligomeric structures of M1. Virology **289:**34–44.
21. **Huang, X., T. Liu, J. Muller, R. A. Levandowski, and Z. Ye.** 2001. Effect of influenza virus matrix protein and viral RNA on ribonucleoprotein formation and nuclear export. Virology **287:**405–416.
22. **Hughey, P. G., P. C. Roberts, L. J. Holsinger, S. L. Zebedee, R. A. Lamb, and R. W. Compans.** 1995. Effects of antibody to the influenza A virus M2 protein on M2 surface expression and virus assembly. Virology **212:**411–421.
23. **Hui, E. K., S. Barman, T. Y. Yang, and D. P. Nayak.** 2003. Basic residues of the helix six domain of influenza virus M1 involved in nuclear translocation of M1 can be replaced by PTAP and YPDL late assembly domain motifs. J. Virol. **77:**7078–7092.
24. **Jasenosky, L. D., G. Neumann, I. Lukashevich, and Y. Kawaoka.** 2001. Ebola virus VP40-induced particle formation and association with the lipid bilayer. J. Virol. **75:**5205–5214.
25. **Jin, H., G. P. Leser, J. Zhang, and R. A. Lamb.** 1997. Influenza virus hemagglutinin and neuraminidase cytoplasmic tails control particle shape. EMBO J. **16:**1236–1247.
26. **Justice, P. A., W. Sun, Y. Li, Z. Ye, P. R. Grigera, and R. R. Wagner.** 1995. Membrane vesiculation function and exocytosis of wild-type and mutant matrix proteins of vesicular stomatitis virus. J. Virol. **69:**3156–3160.
27. **Karacostas, V., K. Nagashima, M. A. Gonda, and B. Moss.** 1989. Human immunodeficiency virus-like particles produced by a vaccinia virus expression vector. Proc. Natl. Acad. Sci. USA **86:**8964–8967.
28. **Kilbourne, E. D., and J. S. Murphy.** 1960. Genetic studies of influenza viruses. I. Viral morphology and growth capacity as exchangeable genetic traits: rapid in ovo adaptation of early passage Asian strain isolates by combination with PR8. J. Exp. Med. **111:**387–406.
29. **Kilbourne, E. D., J. L. Schulman, G. C. Schild, G. Schloer, J. Swanson, and D. Bucher.** 1971. Related studies of a recombinant influenza-virus vaccine. I. Derivation and characterization of virus and vaccine. J. Infect. Dis. **124:**449–462.
30. **Kretzschmar, E., M. Bui, and J. K. Rose.** 1996. Membrane association of influenza virus matrix protein does not require specific hydrophobic domains or the viral glycoproteins. Virology **220:**37–45.
31. **Latham, T., and J. M. Galarza.** 2001. Formation of wild-type and chimeric influenza virus-like particles following simultaneous expression of only four structural proteins. J. Virol. **75:**6154–6165.
32. **Liu, T., and Z. Ye.** 2002. Restriction of viral replication by mutation of the influenza virus matrix protein. J. Virol. **76:**13055–13061.
33. **Mahy, B. W. J.** 1983. Mutants of influenza virus, p. 192–254. *In* P. Palese and D. W. Kingsbury, (ed.), Genetics of influenza viruses. Springer-Verlag, New York, N.Y.
34. **Martin, K., and A. Helenius.** 1991. Nuclear transport of influenza virus ribonucleoproteins: the viral matrix protein (M1) promotes export and inhibits import. Cell **67:**117–130.
35. **Martin, K., and A. Helenius.** 1991. Transport of incoming influenza virus nucleocapsids into the nucleus. J. Virol. **65:**232–244.
36. **Mitnaul, L. J., M. R. Castrucci, K. G. Murti, and Y. Kawaoka.** 1996. The cytoplasmic tail of influenza A virus neuraminidase (NA) affects NA incorporation into virions, virion morphology, and virulence in mice but is not essential for virus replication. J. Virol. **70:**873–879.
37. **Mosley, V. M., and R. W. G. Wyckoff.** 1946. Electron micrography of the virus of influenza. Nature **157:**263.
38. **Muraki, Y., H. Washioka, K. Sugawara, Y. Matsuzaki, E. Takashita, and S. Hongo.** 2004. Identification of an amino acid residue on influenza C virus M1 protein responsible for formation of the cord-like structures of the virus. J. Gen. Virol. **85:**1885–1893.
39. **Nermut, M. V.** 1972. Further investigation on the fine structure of influenza virus. J. Gen. Virol. **17:**317–331.
40. **Neumann, G., T. Watanabe, H. Ito, S. Watanabe, H. Goto, P. Gao, M. Hughes, D. R. Perez, R. Donis, E. Hoffmann, G. Hobom, and Y. Kawaoka.** 1999. Generation of influenza A viruses entirely from cloned cDNAs. Proc. Natl. Acad. Sci. USA **96:**9345–9350.
41. **Patterson, S., J. Gross, and J. S. Oxford.** 1988. The intracellular distribution of influenza virus matrix protein and nucleoprotein in infected cells and their relationship to haemagglutinin in the plasma membrane. J. Gen. Virol. **69:**1859–1872.
42. **Pornillos, O., J. E. Garrus, and W. I. Sundquist.** 2002. Mechanisms of enveloped RNA virus budding. Trends Cell Biol. **12:**569–579.
43. **Rees, P. J., and N. J. Dimmock.** 1981. Electrophoretic separation of influenza virus ribonucleoproteins. J. Gen. Virol. **53:**125–132.
44. **Roberts, P. C., R. A. Lamb, and R. W. Compans.** 1998. The M1 and M2 proteins of influenza A virus are important determinants in filamentous particle formation. Virology **240:**127–137.
45. **Ruigrok, R. W., L. J. Calder, and S. A. Wharton.** 1989. Electron microscopy of the influenza virus submembranal structure. Virology **173:**311–316.
46. **Schmitt, A. P., and R. A. Lamb (ed.).** 2004. Escaping from the cell: assembly and budding of negative-strand RNA viruses. Curr. Top. Microbiol. Immunol. **283:**145–196.

47. **Schulze, I. T.** 1972. The structure of influenza virus. II. A model based on the morphology and composition of subviral particles. Virology **47:**181–196.
48. **Sha, B., and M. Luo.** 1997. Structure of a bifunctional membrane-RNA binding protein, influenza virus matrix protein M1. Nat. Struct. Biol. **4:**239–244.
49. **Smirnov Yu, A., M. A. Kuznetsova, and N. V. Kaverin.** 1991. The genetic aspects of influenza virus filamentous particle formation. Arch. Virol. **118:** 279–284.
50. **Timmins, J., S. Scianimanico, G. Schoehn, and W. Weissenhorn.** 2001. Vesicular release of Ebola virus matrix protein VP40. Virology **283:**1–6.
51. **Wakefield, L., and G. G. Brownlee.** 1989. RNA-binding properties of influenza A virus matrix protein M1. Nucleic Acids Res. **17:**8569–8580.
52. **Watanabe, K., H. Handa, K. Mizumoto, and K. Nagata.** 1996. Mechanism for inhibition of influenza virus RNA polymerase activity by matrix protein. J. Virol. **70:**241–247.
53. **Whittaker, G., M. Bui, and A. Helenius.** 1996. Nuclear trafficking of influenza virus ribonucleoproteins in heterokaryons. J. Virol. **70:**2743–2756.
54. **Whittaker, G., I. Kemler, and A. Helenius.** 1995. Hyperphosphorylation of mutant influenza virus matrix protein, M1, causes its retention in the nucleus. J. Virol. **69:**439–445.
55. **Ye, Z., T. Liu, D. P. Offringa, J. McInnis, and R. A. Levandowski.** 1999. Association of influenza virus matrix protein with ribonucleoproteins. J. Virol. **73:**7467–7473.
56. **Ye, Z., D. Robinson, and R. R. Wagner.** 1995. Nucleus-targeting domain of the matrix protein (M1) of influenza virus. J. Virol. **69:**1964–1970.
57. **Ye, Z. P., N. W. Baylor, and R. R. Wagner.** 1989. Transcription-inhibition and RNA-binding domains of influenza A virus matrix protein mapped with anti-idiotypic antibodies and synthetic peptides. J. Virol. **63:**3586–3594.
58. **Ye, Z. P., R. Pal, J. W. Fox, and R. R. Wagner.** 1987. Functional and antigenic domains of the matrix (M1) protein of influenza A virus. J. Virol. **61:**239–246.
59. **Zhang, J., and R. A. Lamb.** 1996. Characterization of the membrane association of the influenza virus matrix protein in living cells. Virology **225:**255–266.
60. **Zhang, J., G. P. Leser, A. Pekosz, and R. A. Lamb.** 2000. The cytoplasmic tails of the influenza virus spike glycoproteins are required for normal genome packaging. Virology **269:**325–334.
61. **Zhang, J., A. Pekosz, and R. A. Lamb.** 2000. Influenza virus assembly and lipid raft microdomains: a role for the cytoplasmic tails of the spike glycoproteins. J. Virol. **74:**4634–4644.
62. **Zvonarjev, A. Y., and Y. Z. Ghendon.** 1980. Influence of membrane (M) protein on influenza A virus virion transcriptase activity in vitro and its susceptibility to rimantadine. J. Virol. **33:**583–586.